Hindawi
Discrete Dynamics in Nature and Society
Volume 2022, Article ID 8395116, 8 pages
https://doi.org/10.1155/2022/8395116

Research Article

Evaluation of the Mechanical Failure Criterion to Consider the Triple Base Propellant Safety Life: Application of Sustainable Renewables for Environmental Hazards

Liqian Song,[1] Yan Wang,[2] Dabin Liu,[1] Hua Qian,[1] Xiaoting Rui,[2] and M. Mehdi Shafieezadeh[3]

[1]*School of Chemistry and Chemical Engineering, Nanjing University of Science and Technology, Nanjing 210000, Jiangsu, China*
[2]*Institute of Launch Dynamics, Nanjing University of Science and Technology, Nanjing 210000, Jiangsu, China*
[3]*Department of Chemical Engineering, Islamic Azad University, Shiraz Branch, Iran*

Correspondence should be addressed to Dabin Liu; liu2008235@163.com and M. Mehdi Shafieezadeh; shafieenezhad.shirazu@gmail.com

Received 31 July 2022; Revised 26 August 2022; Accepted 5 September 2022; Published 22 September 2022

Academic Editor: Reza Lotfi

Implementation of clean energy and renewables is essential for the consideration of environmental impact because it can be implemented in supply chain networks and sustainable management procedures for safety. In order to study the safety life failure criterion of a triple base propellant under the failure mode of mechanical properties, an accelerated aging test, an evaluation method for the launch safety test of gun propellant charge, and a compressive strength test were used. The failure criterion of mechanical properties was obtained by researching the correlation between launch safety change and mechanical property change of samples. Berthelot's equation was used to predict the safety life of the triple base propellant. The results show that the mechanical failure criterion is "27% reduction of maximum compressive strength." The safety life at 25°C and 75% humidity is 13.77 years.

1. Introduction

As the power source of ammunition, the performance of the propellant directly affects the operational efficiency of the ammunition system [1–6]. With the rapid development of military technology, the speed of equipment upgrading is increasing faster and faster, and new propellants are emerging indefinitely [7–11]. The triple base propellant is a kind of high-energy propellant, which is widely used in large caliber ammunition systems [12–16]. Compared with the traditional propellant, its composition is more complex [17–21]. The use of new materials and new technologies leads to the degradation law and mechanism of the propellant in the long-term storage process, which is significantly different from the traditional propellant [22–27]. Triple base propellants have the characteristics of high energy, high burning rate, and low burning temperature because of the addition of nitramine azide as an energetic plasticizer [28, 29]. Due to the complex composition and variety of influencing factors in the process of storage and use, there are few research studies on its safety life [30–33] and mainly focus on the change of the content of stabilizers during storage [34–37]. Accidents such as early explosion or chamber explosion occur in the use of a triple base propellant, which is still in the safe life range [38–41]. This indicates that the safety life assessment of a triple base propellant based on the content of the stabilizer is defective. If the mechanical failure criterion can be determined by some method, the accuracy and efficiency of the triple base propellant life assessment will be greatly improved.

The triple base propellant was mainly affected by the mechanical environment of the chamber in the process of use. Due to the high-speed and high-pressure combustion gas in the chamber, propellant particles will be squeezed and

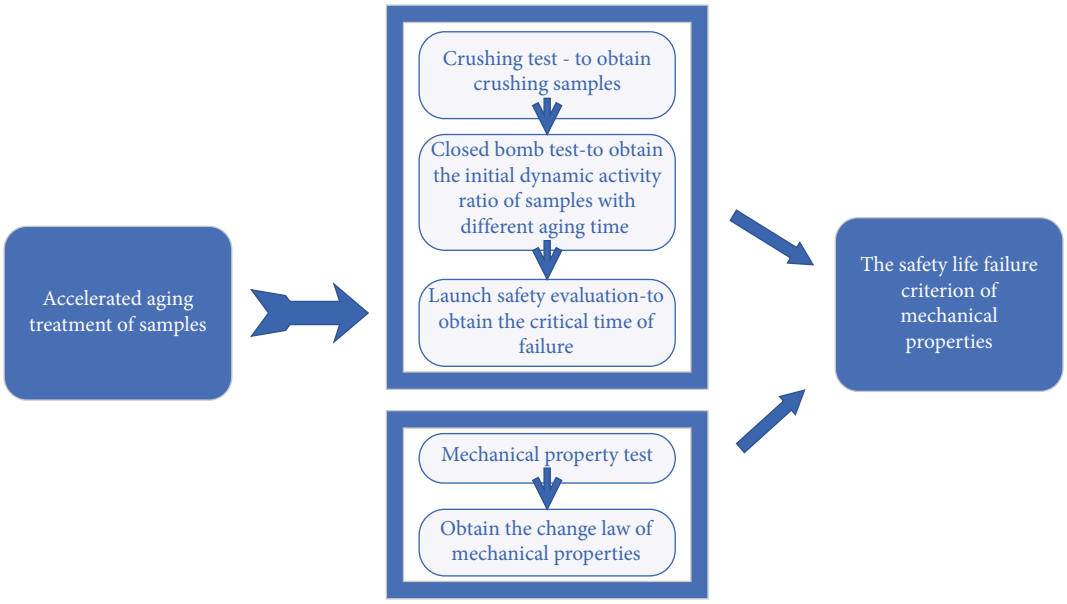

Figure 1: Flowchart of the experimental scheme.

collide with each other during the launching process, and they will also be strongly impacted by the bottom and wall of the shell. Many fragmentations are made when the mechanical conditions of propellant particles cannot meet the requirements of the strong load in the chamber, which will lead to a sharp increase in the burning surface and the gas generation rate of the propellant. This can lead to a sudden increase in local pressure in the chamber and eventually lead to premature explosion or even chamber explosion [42, 43]. Therefore, the mechanical properties of triple base propellants are the key factors affecting the safe use of samples after long-term storage. Research shows that the change of mechanical properties is the main feature of the storage process of triple base propellants, and tracking the change of mechanical properties can directly reflect the performance of triple base propellants. But due to the lack of failure criteria, the life evaluation parameters cannot be obtained directly according to the data of mechanical properties [44].

The dynamic process of propellants in the process of launching can be simulated by the "evaluation method for launch safety test of gun propellant charge" [45], which accurately judges whether the sample meets the safety requirements for launching. However, the aging life of samples cannot be obtained quickly because of the large number of test samples and long test cycles. Based on the respective characteristics of the mechanical performance test of triple base propellants and the launch safety test of propellants, whether the two can be combined to obtain the mechanical failure criterion of triple base propellants and establish the mechanical aging life evaluation method of triple base propellants is of great significance to solve the safety life problem of triple base propellants in the service process.

In this study, the mechanical test and the launch safety test were carried out to explore the correlation between static mechanical property and launch safety. The obtained mechanical property change data are correlated with the launch safety test data to obtain the mechanical property failure critical point of triple base propellants. The aging life equation of propellants under a mechanical failure mode was established, and the safety life of triple base propellants is estimated based on the determined failure criterion.

2. Experimental

2.1. Experimental Scheme. The experimental scheme is shown in Figure 1.

2.2. Accelerated Aging Test. In order to shorten the test period, the samples of triple base propellants with different aging degrees were obtained by an accelerated aging test. The accelerated aging test conditions refer to the national military standard GJB 770B-05 [46].

Aging temperature is as follows: 51°C, 61°C, and 71°C.

Aging humidity is as follows: 75% (annual average humidity of the test site).

2.3. Mechanical Property Test. The precision universal material testing machine was used to test the compressive strength according to "method 415.1", GJB770B-05.

2.4. Launch Safety Test. The launch safety test can reproduce the combustion and mechanical environment in the propellant chamber, simulate the extrusion crushing dynamic process of the propellant charge in the launching environment according to the chamber explosion mechanism of the propellant charge, and finally establish the quantitative relationship between the extrusion stress of the propellant and the crushing degree in the corresponding launching environment [47].

Table 1: The calibration data of the test device.

	Maximum bottom pressure/MPa	Initial velocity of projectile/ $m \cdot s^{-1}$
Simulation	331.0	929.6
Test	327.4	931.0
Error*	1.1%	0.16%

*Error value = |(Simulation value) − (Test value)/Simulation value × 100%|.

(a) (b) (c)

Figure 2: Broken samples of different aging times under the same pressure; (a) samples without storage; (b) samples aged for 15 days; (c) samples aged for 30 days.

2.4.1. Evaluation Process

(1) The [48–50] extrusion crushing process of projectile bottom propellant charge during gun launching is simulated by the extrusion crushing simulation test device of propellant charge, and the broken propellant bed of propellant charge under the extrusion stress of projectile bottom propellant charge is obtained.

(2) The dynamic activity test of the broken propellant bed is carried out by using the dynamic activity test system of propellant charge, and the dynamic activity curve and the initial dynamic activity ratio of the projectile bottom broken propellant bed under real launch conditions and mechanical environment are determined.

(3) The critical initial activity ratio is determined according to the extrusion stress of the projectile bottom in the actual launching of the propellant, which is used as the evaluation standard.

3. Analysis of Test Results

3.1. Results of the Launch Safety Test. After the accelerated aging test, the broken propellant in the real mechanical environment is obtained by using the overload simulation loading device. The initial dynamic activity ratio of the broken propellant with different aging times was obtained by the initial dynamic activity ratio test. The calibration data of the test device are shown in Table 1.

The errors between the simulated parameters of the test device and the actual launch environment parameters meet the test requirements after correction.

3.1.1. Results of the Crushing Test. In order to obtain the relationship between the initial dynamic activity ratio and aging time of samples, it is necessary to conduct dynamic activity ratio tests on broken samples with different aging times and different test pressures. The first step of the whole experiment is to obtain samples with different degrees of fragmentation. The broken samples with different aging times are obtained by using the overload simulation loading device. The test results are shown in Figure 2, Tables 2–4.

Table 2: Test data of propellant fragmentation without storage.

No.	Weight/ g	Maximum extrusion stress of the propellant bed/ MPa
1	198.5	7.20
2	198.5	10.59
3	201.5	15.63

Table 3: Fragmentation test data of propellant samples aged for 15 days.

No.	Weight/ g	Maximum extrusion stress of the propellant bed/ MPa
1	199.5	5.97
2	203.5	9.12
3	203.0	14.38

Table 4: Fragmentation test data of propellant samples aged for 30 days.

No.	Weight/ g	Maximum extrusion stress of the propellant bed/ MPa
1	202.5	7.843
2	203.5	10.28
3	202.5	15.36

From the test results, it can be seen that the crushing degree of samples with the same aging time increases with the maximum pressure of the simulated device bed. The crushing degree of samples increases with aging time. This shows that the mechanical properties of the samples are decreased after aging.

3.1.2. Dynamic Activity Ratio Test. The P-t curve shows the change of pressure in the test equipment with time and can

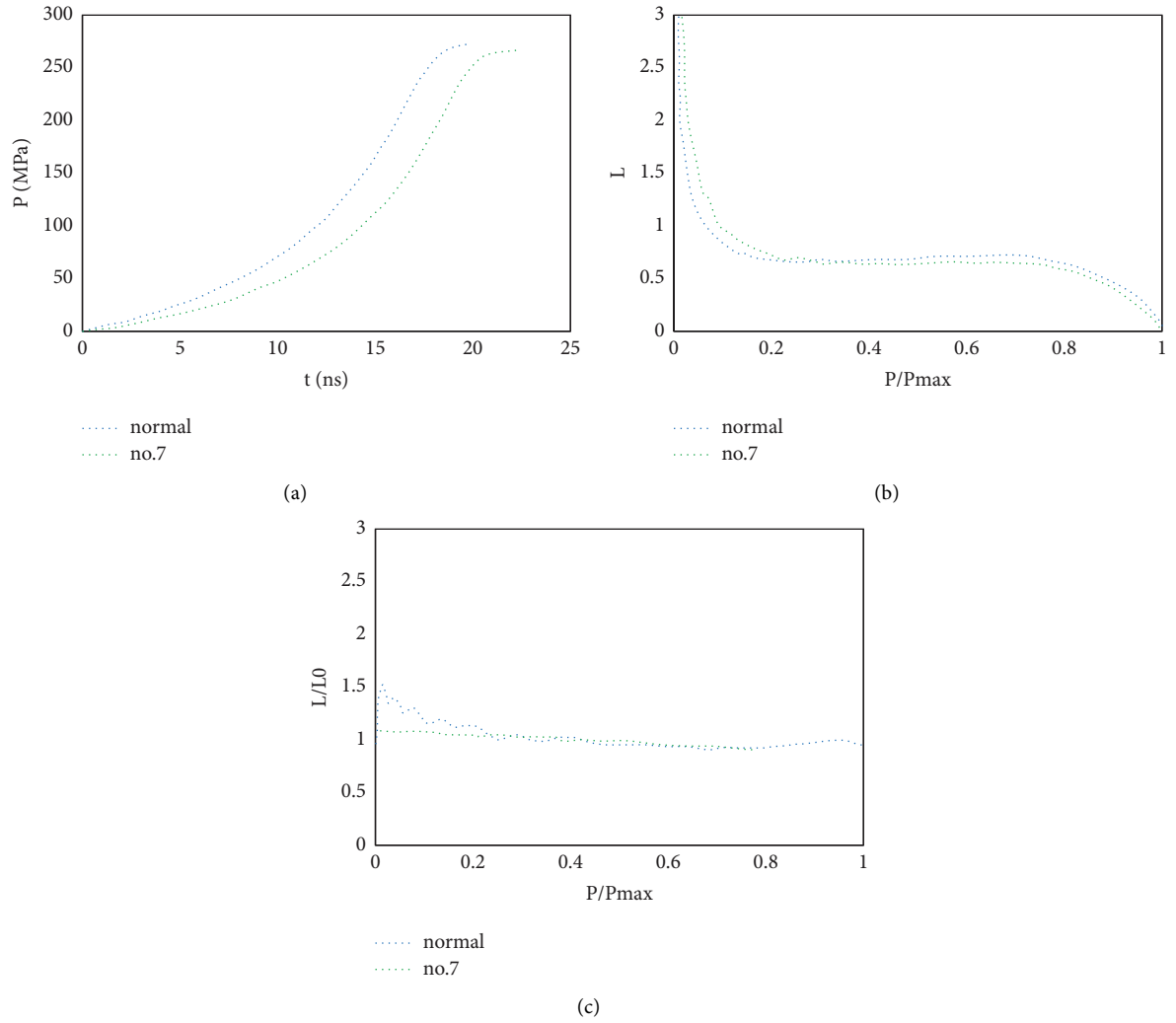

Figure 3: P-t curves, dynamic activity curves, and dynamic activity ratio curves of propellants. (a) P-t curves, (b) dynamic activity curves, and (c) dynamic activity ratio curves.

Table 5: Test data of the initial dynamic activity ratio of samples without storage.

No.	Weight/g	Maximum extrusion stress of the propellant bed/MPa	Initial dynamic activity ratio/R_0
1	198.5	7.20	1.024
2	198.5	10.59	1.084
3	201.5	15.63	1.108

Table 6: Test data of the initial dynamic activity ratio of samples aged for 15 days.

No.	Weight/g	Maximum extrusion stress of the propellant bed/MPa	Initial dynamic activity ratio/R_0
1	199.5	5.97	1.198
2	203.5	9.12	1.259
3	203.0	14.38	1.519

reflect the acceleration of the initial combustion rate and the gas production rate caused by the increase of the combustion surface after the sample is broken. The dynamic activity curve can be further obtained through the P-t curve, and the initial dynamic activity ratio data and curves are obtained as shown in Figure 3.

The test data of different samples are shown in Table 5, Table 6, and Table 7.

Composed the diagram from the test data.

Figure 4 shows that the dynamic initial activity ratio increases with the increase of the maximum bed pressure at the same aging time. The longer the aging time of the sample, the

Table 7: Test data of the initial dynamic activity ratio of samples aged for 30 days.

No.	Weight/g	Maximum extrusion stress of the propellant bed/MPa	Initial dynamic activity ratio/R_0
1	202.5	7.843	1.374
2	203.5	10.28	1.427
3	202.5	15.36	1.661

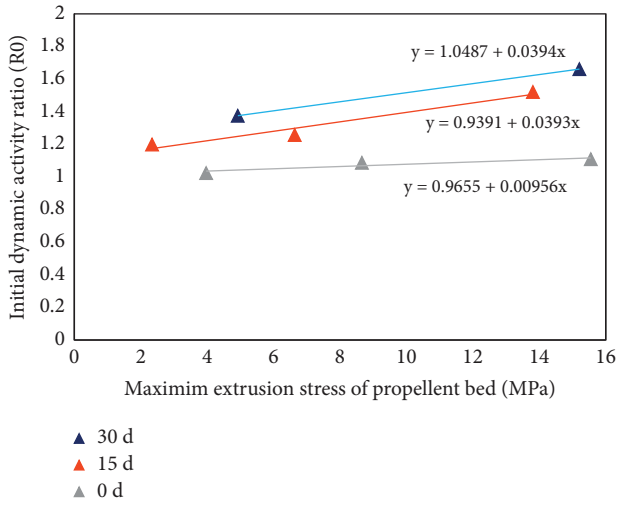

Figure 4: The initial dynamic activity ratio of samples with different aging times.

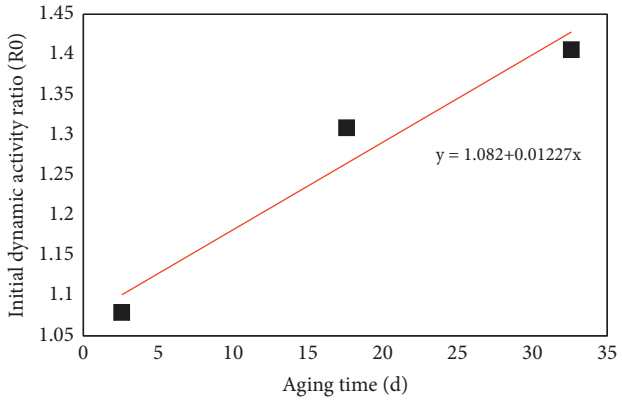

Figure 5: Dynamic initial activity ratio-aging time curve.

greater the fragmentation, and the greater the dynamic initial activity ratio, the higher the maximum bed pressure. The test results show that the maximum pressure of a gun barrel is 9.58 Mpa, and the corresponding dynamic initial activity ratios of propellant samples with different aging times are 1.057, 1.316, and 1.425, respectively. According to the data, we make a curve of dynamic initial activity ratio aging times, as shown in Figure 5.

According to the "evaluation method for the launch safety test of gun propellant charge," when $R_0 < 1.3$, the samples are safe to launch. From the fitting equation "y = 1.082 + 0.01227x (R^2 = 96%)," when $y = 1.3$, $x = 17.76$. In other words, when accelerated at 71°C for 17 days, the launch safety reaches the critical point.

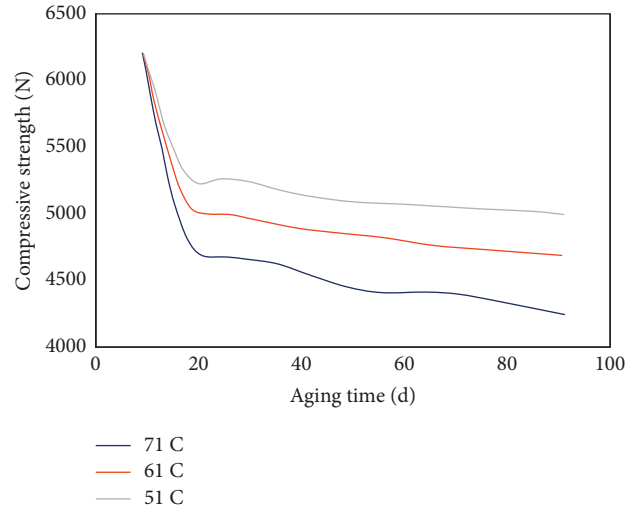

Figure 6: Change curves of compressive strength with aging time.

3.2. Compressive Strength Test. In this study, the maximum compressive strength of the samples was obtained by measuring the propellant samples with different aging times. Taking $F = 6200$ N as the starting point (average compressive strength of the nonaged sample at room temperature), according to the original data, the curves of compressive strength with aging time were obtained, as shown in Figure 6.

It can be seen from Figure 6 that the compressive strength of propellant samples decreases with the increase of aging time at different aging temperatures; at the same aging temperature, the greater the humidity is, the faster the compressive strength decreases. This may be due to the degradation and chain breakage of polymers such as nitrocellulose. The grid structure formed by nitrocellulose is damaged, and the overall mechanical strength is reduced [51, 52]. In addition, in an environment of high humidity and high temperature, the droplets condensed on the surface of the pillar will dissolve some components such as nitroguanidine, and the greater the humidity, the greater the dissolution. This will result in loosening of the overall structure of the propellant column and formation of ravines and holes on the surface, weakening the integrity of the overall structure of the propellant. Furthermore, under the action of stress, the surface layer structure is easy to deform, resulting in a decrease in the overall compressive strength.

3.3. Mechanical Life Evaluation Equation. MATLAB software was used to fit the compressive strength of samples at different aging temperatures. First, we define the values of x and y, i.e., $x = t(\ldots)$ and $y = F(\ldots)$ and then output the curve. We select the classical equation in the function library to

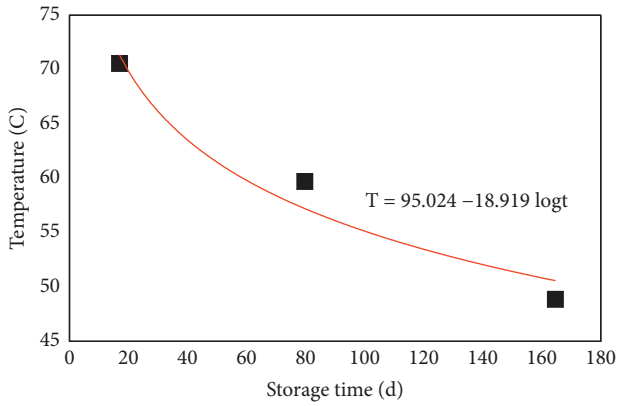

Figure 7: Life fitting curve.

Table 8: Aging time to failure critical point under different aging conditions.

Aging temperature/T	51°C (d)	61°C (d)	71°C (d)
Aging time/t	174	84	17

The life evaluation equation is obtained by using the Berthelot equation of fit.

simulate the curve, and the following equation can be obtained.

$T = 51^{\circ}C$:

$$F = 5173 \times \exp(-0.0007781t)\left(R^2 = 96\%\right), \quad (1)$$

$T = 61^{\circ}C$:

$$F = 4930 \times \exp(-0.001041t)\left(R^2 = 96\%\right), \quad (2)$$

$T = 71^{\circ}C$:

$$F = 4650 \times \exp(-0.001704t)\left(R^2 = 95\%\right). \quad (3)$$

F is the maximum compressive strength, N; t is the storage time, d.

It can be seen from the launch safety test that the sample reaches the critical point of launch safety after 17 days of aging under the conditions of the 71°C accelerated aging test. When $t = 17$ is taken into (2), $F = 4517$N. The decrease degree of the maximum compressive strength can be determined by $\alpha = (1\text{-}F/6200) \times 100\%$, and then $\alpha = 27.15\% \approx 27\%$. Under the accelerated aging test condition, when the maximum compressive strength of the sample decreases by 27%, the critical point of launch safety is reached, which is the mechanical failure criterion. According to formula (1–3), the aging time of samples reaching the critical point of failure under accelerated aging test conditions at different temperatures can be obtained based on the criterion of 27% reduction of maximum compressive strength, as shown in figure 7, Table 8.

$$(T = 95.024 - 18.919 \log t)\left(R^2 = 96\%\right). \quad (4)$$

T is the aging temperature, °C; t is the storage time, d.

According to the mechanical failure criterion "the maximum compressive strength decreases by 27%," and the life of the triple base propellant is evaluated. According to (4), when $t = 25^{\circ}C$, the storage time is 5026 days, that is, the safe life of the triple base propellant is 13.77 years at room temperature (25°C).

4. Discussion and Conclusion

4.1. Discussion. This study shows the correlation between mechanical properties and launch safety. The combination of the two test methods has solved the problem that the triple base propellant lacks the mechanical failure criterion and cannot be evaluated from the perspective of mechanical properties.

The test results of propellant launching safety show that under the same chamber mechanical environment, the extension of aging time will lead to the increase of triple base propellant fragmentation, the sudden increase of the combustion surface, the acceleration of the initial burning rate, the acceleration of local pressure, and the increase of the dynamic initial activity ratio. The mechanical test shows that the maximum compressive strength of the triple base propellant decreases with aging time; at the same aging time, the higher the aging temperature is, the faster the maximum compressive strength decreases.

The change laws of these experimental phenomena are related. Combined with the data of the 71°C accelerated aging test and the results of the propellant launching safety test, the mechanical failure criterion of the triple base propellant is calculated as "the maximum compressive strength decreases by 27%." Of course, this result may not be accurate and specific, but this method to determine the mechanical failure criterion of the propellant is feasible. In the follow-up study, more accurate and instructive life evaluation results can be obtained by increasing the number of tests and reducing the error.

4.2. Conclusion. The method of combining launching safety tests with mechanical property tests solves the problem that it is difficult to determine the mechanical failure criterion of triple base propellants and provides a strong basis for the establishment of a life evaluation system for such propellants.

(1) The relationship between the aging time and initial dynamic activity ratio in the process of accelerated aging of triple base propellants at 71°C can be expressed by the equation: y = 1.082 + 0.01227x ($R2 = 94\%$). When the dynamic initial activity ratio is 1.3, the aging time is about 17 days.

(2) The mechanical failure criterion of the triple base propellant is calculated as "the maximum compressive strength decreases by 27%." According to the Berthelot equation, the safety life of the triple base propellant at room temperature (25°C) is 13.77 years.

Abbreviations

R_0: Initial dynamic activity ratio
T: Accelerated aging test temperature/°C
F: Maximum compressive strength/N
T: Storage time/days
α: Degradation degree of mechanical properties
R^2: Goodness of fit
P-t: Relationship between pressure and time during the test
L: The value of the dynamic activity
P_{max}: Maximum pressure that the sample can reach during the test/Mpa.

Data Availability

No data were used to support the findings of this study.

Conflicts of Interest

The authors declare no conflicts of interest.

References

[1] Y. Xu, K. Li, J. Hu, and K. Li, "A genetic algorithm for task scheduling on heterogeneous computing systems using multiple priority queues," *Information Sciences*, vol. 270, pp. 255–287, 2014.

[2] J. Chen, K. Li, Z. Tang et al., "A parallel random forest algorithm for big data in a spark cloud computing environment," *IEEE Transactions on Parallel and Distributed Systems*, vol. 28, no. 4, pp. 919–933, 2017.

[3] C. Liu, K. Li, and K. Li, "A game approach to multi-servers load balancing with load-dependent server availability consideration," *IEEE Transactions on Cloud Computing*, vol. 9, no. 1, pp. 1–13, 2021.

[4] G. Xiao, K. Li, Y. Chen, W. He, A. Y. Zomaya, and T. Li, "CASpMV: a customized and accelerative SPMV framework for the sunway TaihuLight," *IEEE Transactions on Parallel and Distributed Systems*, vol. 32, no. 1, pp. 131–146, 2021.

[5] K. Li, W. Yang, and K. Li, "Performance analysis and optimization for SpMV on GPU using probabilistic modeling," *IEEE Transactions on Parallel and Distributed Systems*, vol. 26, no. 1, pp. 196–205, 2015.

[6] J. Chen, X. Zhou, K. Bilal, K. Li, K. Li, and P. S. Yu, "A bi-layered parallel training architecture for large-scale convolutional neural networks," *IEEE Transactions on Parallel and Distributed Systems*, vol. 30, no. 5, pp. 965–976, 2019.

[7] C. Liu, K. Li, K. Li, and R. Buyya, "A new service mechanism for profit optimizations of a cloud provider and its users," *IEEE Transactions on Cloud Computing*, vol. 9, no. 1, pp. 14–26, 2021.

[8] C. Chen, K. Li, W. Wei, J. T. Zhou, and Z. Zeng, "Hierarchical graph neural networks for few-shot learning," *IEEE Transactions on Circuits and Systems for Video Technology*, vol. 32, no. 1, pp. 240–252, 2022.

[9] M. Duan, K. Li, K. Li, and Q. Tian, "A novel multi-task tensor correlation neural network for facial attribute prediction," *ACM Transactions on Intelligent Systems and Technology (TIST)*, vol. 12, no. 1, pp. 1–22, 2021.

[10] C. Chen, K. Li, S. G. Teo, X. Zou, K. Li, and Z. Zeng, "Citywide traffic flow prediction based on multiple gated spatio-temporal convolutional neural networks," *ACM Transactions on Knowledge Discovery from Data*, vol. 14, no. 4, pp. 1–23, 2020.

[11] J. Hu, K. Li, C. Liu, and K. Li, "A game-based price bidding algorithm for multi-attribute cloud resource provision," *IEEE Transactions on Services Computing*, vol. 14, no. 4, pp. 1111–1122, 2021.

[12] J. Chen, K. Li, K. Li, P. S. Yu, and Z. Zeng, "Dynamic planning of bicycle stations in dockless public bicycle-sharing system using gated graph neural network," *ACM Transactions on Intelligent Systems and Technology (TIST)*, vol. 12, no. 2, pp. 1–22, 2021.

[13] B. Pu, K. Li, S. Li, and N. Zhu, "Automatic fetal ultrasound standard plane recognition based on deep learning and IIoT," *IEEE Transactions on Industrial Informatics*, vol. 17, no. 11, pp. 7771–7780, 2021.

[14] K. Li, X. Tang, and K. Li, "Energy-efficient stochastic task scheduling on heterogeneous computing systems," *IEEE Transactions on Parallel and Distributed Systems*, vol. 25, no. 11, pp. 2867–2876, 2014.

[15] Y. Chen, K. Li, W. Yang, G. Xiao, X. Xie, and T. Li, "Performance-aware model for sparse matrix-matrix multiplication on the sunway taihulight supercomputer," *IEEE Transactions on Parallel and Distributed Systems*, vol. 30, no. 4, pp. 923–938, 2019.

[16] K. Li, X. Tang, B. Veeravalli, and K. Li, "Scheduling precedence constrained stochastic tasks on heterogeneous cluster systems," *IEEE Transactions on Computers*, vol. 64, no. 1, pp. 191–204, 2015.

[17] M. Duan, K. Li, X. Liao, and K. Li, "A parallel multiclassification algorithm for big data using an extreme learning machine," *IEEE Transactions on Neural Networks and Learning Systems*, vol. 29, no. 6, pp. 2337–2351, 2018.

[18] X. Zhou, K. Li, Y. Zhou, and K. Li, "Adaptive processing for distributed skyline queries over uncertain data," *IEEE Transactions on Knowledge and Data Engineering*, vol. 28, no. 2, pp. 371–384, 2016.

[19] J. Wang, C. Ju, Y. Gao, A. K. Sangaiah, and G. J. Kim, "A PSO based energy efficient coverage control algorithm for wireless sensor networks," *Computers, Materials & Continua*, vol. 56, no. 3, pp. 433–446, 2018.

[20] J. Wang, Y. Gao, X. Yin, F. Li, and H. J. Kim, "An enhanced PEGASIS algorithm with mobile sink support for wireless sensor networks," *Wireless Communications and Mobile Computing*, vol. 2018, Article ID 9472075, 2018.

[21] Z. Liao, J. Wang, S. Zhang, J. Cao, and G. Min, "Minimizing movement for target coverage and network connectivity in mobile sensor networks," *IEEE Transactions on Parallel and Distributed Systems*, vol. 26, no. 7, pp. 1971–1983, 2015.

[22] J. Wang, Y. Gao, W. Liu, A. K. Sangaiah, and H. J. Kim, "An intelligent data gathering schema with data fusion supported for mobile sink in wireless sensor networks," *International Journal of Distributed Sensor Networks*, vol. 15, no. 3, Article ID 155014771983958, 2019.

[23] J. Zhang, X. Jin, J. Sun, J. Wang, and A. K. Sangaiah, "Spatial and semantic convolutional features for robust visual object tracking," *Multimedia Tools and Applications*, vol. 79, no. 21-22, pp. 15095–15115, 2020.

[24] F. Yu, L. Liu, L. Xiao, K. Li, and S. Cai, "A robust and fixed-time zeroing neural dynamics for computing time-variant nonlinear equation using a novel nonlinear activation function," *Neurocomputing*, vol. 350, pp. 108–116, 2019.

[25] J. Wang, X. Gu, W. Liu, A. K. Sangaiah, and H. J. Kim, "An empower Hamilton loop based data collection algorithm with

mobile agent for WSNs," *Human-centric Computing and Information Sciences*, vol. 9, no. 1, pp. 18–14, 2019.

[26] L. Xiang, X. Shen, J. Qin, and W. Hao, "Discrete multi-graph hashing for large-scale visual search," *Neural Processing Letters*, vol. 49, no. 3, pp. 1055–1069, 2019.

[27] Y. Bai, D. C. Nardi, X. Zhou, R. A. Picón, and J. Flórez-López, "A new comprehensive model of damage for flexural subassemblies prone to fatigue," *Computers & Structures*, vol. 256, Article ID 106639, 2021.

[28] J. L Wang, Y. P. Ji, F. L Gao, W. Guo, and S. T. Ren, "Experimental measurement of safety parameters of DIANP," *Chinese Journal of Energetic Materials*, vol. 19, no. 6, pp. 693–696, 2011.

[29] Z. Huang, J. Fan, and Y. Chen, "Experimental study on the surface deterring of azidonitramine gun propellant [J]," *Chinese Journal of Explosives and Propellants*, vol. 36, no. 2, pp. 62–64, 2013.

[30] X. Liao, P. Du, and Z. Wang, "Service life of RB nitramine propellant," *Chinese Journal of Energetic Materials*, vol. 20, no. 2, pp. 188–191, 2010.

[31] S. Heng, F. Han, L. Zhang, J. Liu, and Y. Pu, "Estimation method and results of safe storage life for nitrate ester propellants," *Chinese Journal of Explosives and Propellants*, vol. 29, no. 4, pp. 71–76, 2006.

[32] B. Roduit, M. Hartmann, P. Folly, A. Sarbach, and R Baltensperger, "Prediction of thermal stability of materials by modified kinetic and model selection approaches based on limited amount of experimental points," *Thermochimica Acta*, vol. 579, pp. 31–39, 2014.

[33] Y. Gu, D.-mei Zhang, L. Zhang, and Q. Wang, "Method of predicting the storage life of a tri-base gun propellant[J]," *Chinese Journal of Explosives and Propellants*, vol. 40, no. 1, pp. 91–96, 2017.

[34] H. Chen, Y. Xiong, S. Li, Z. Song, Z. Hu, and F. Liu, "Multi-Sensor data driven with PARAFAC-IPSO-PNN for identification of mechanical nonstationary multi-fault mode," *Machines*, vol. 10, no. 2, p. 155, 2022.

[35] H. Chen and S. Li, "Multi-Sensor fusion by CWT-PARAFAC-IPSO-SVM for intelligent mechanical fault diagnosis," *Sensors*, vol. 22, no. 10, p. 3647, 2022.

[36] L. Zhang, H. Zhang, and G. Cai, "The multi-class fault diagnosis of wind turbine bearing based on multi-source signal fusion and deep learning generative model," *IEEE Transactions on Instrumentation and Measurement*, vol. 71, 12 pages, 2022.

[37] W. Liu, L. Liu, H. Wu et al., "Performance analysis and offshore applications of the diffuser augmented tidal turbines," *Ships and Offshore Structures*, pp. 1–10, 2022.

[38] Z. j. Wang and H. f. Qiang, "Mechanical properties of thermal aged HTPB composite solid propellant under confining pressure," *Defence technology*, vol. 18, no. 4, pp. 618–625, 2022.

[39] Z. Wang, H. Qiang, J. Wang, and L. Duan, "Experimental investigation on fracture properties of HTPB propellant with circumferentially notched cylinder sample," *Propellants, Explosives, Pyrotechnics*, vol. 47, no. 7, Article ID e202200046, 2022.

[40] K. Wang, Z. Zhang, P. Yang, and H. Teng, "Numerical study on reflection of an oblique detonation wave on an outward turning wall," *Physics of Fluids*, vol. 32, no. 4, Article ID 46101, 2020.

[41] K. Wang, H. Teng, P. Yang, and H. D. Ng, "Numerical investigation of flow structures resulting from the interaction between an oblique detonation wave and an upper expansion corner," *Journal of Fluid Mechanics*, vol. 903, 2020.

[42] L. Song, D. Liu, H. Qian, and B. Liu, "Aging life evaluation of a tri-base gun propellant," *Chinese Journal of Explosives and Propellants*, vol. 41, no. 6, pp. 627–631, 2018.

[43] Y. Chen, X. Luo, J. Zhen, G. Liu, and G. Wang, "Mechanical properties of granular gun propellant," *Chinese Journal of Explosives and Propellants*, vol. 36, no. 6, pp. 82–85, 2013.

[44] X. Rui, *Introduction to Ammunition Launching Safety*, National Defense Industry Press, London, UK, 2009.

[45] X. Rui, B. Feng, Y. Wang, Li Chao, and T. Chen, "Research on evaluation method for launch safety of propellant charge," *Acta Armamentarii*, vol. 36, no. 1, pp. 1–11, 2015.

[46] COSTINDWJB, *770B-2005 Test Method of propellant*, Publication Department of COSTIND, Beijing, China, 2005.

[47] X. Rui, Y. Wang, and G. Wang, "Advances in test method of launch safety of ammunition," *Ordnance Industry Automation*, vol. 31, no. 12, pp. 81–84, 2012.

[48] X. Rui, B. Feng, and G. Wang, "Evaluation method of launch safety of propellant charge," *Ordnance Industry Automation*, vol. 30, no. 5, pp. 56–59, 2011.

[49] X. Rui, L. Yun, S. Nansheng, T. Chen, H. Wang, and J. Liu, "Advance on launch safety for gun propellant charge," *Acta Armamentarii*, vol. 26, no. 5, pp. 690–696, 2005.

[50] W. J. Costind, *20390.8-2016 Evaluation Method for Launch Safety Test of Gun Propellant charge*, Publication Department of COSTIND, Beijing, China, 2016.

[51] Y. Yao, F. Wang, Y. Zhang, W. Lun, and H. Yu, "Study on improving mechanical properties of new high energy propellant," *Metrology & Measurement Technology*, vol. 33, no. S1, pp. 132-133, 2013.

[52] X. Qi, X. Zhang, Q. Yan, and Mi Hu, "Temperature dependence of mechanical state for nitrocellulose/nitroglycerin blend," *Journal of Propulsion Technology*, vol. 37, no. 7, pp. 1387–1392, 2016.